MyoVibe: Vibration Based Wearable Muscle Activation Detection In High Mobility Exercises

Frank Mokaya†, Roland Lucas⊕, Hae Young Noh† and Pei Zhang†
†Carnegie Mellon University, ⊕Lucas Physical Therapy & Fitness
fmokaya@cmu.edu, manualphysio@gmail.com, noh@cmu.edu, peizhang@cmu.edu

ABSTRACT
Skeletal muscles are activated to generate the force needed for movement in most high motion sports and exercises. However, incorrect skeletal muscle activation during these sports and exercises, can lead to sub-optimal performance and injury. Existing techniques are susceptible to motion artifacts, particularly when used in high motion sports (e.g. jumping, cycling, etc.). They require limited body movement, or experts to manually interpret results, making them unsuitable in sports scenarios.

This paper presents MyoVibe, a wearable system for determining muscle activation in high motion exercise scenarios. MyoVibe senses muscle vibration signals obtained from a wearable network of accelerometers to determine muscle activation. By modeling the characteristics of muscles and high motion noise using extreme value analysis, MyoVibe can reduce noise due to high mobility exercises. Our system can predict muscle activation with greater than 97% accuracy in isometric low motion exercise cases, up to 90% accuracy in high motion exercises.

ACM Classification Keywords
J.3 Life and Medical Sciences: Medical information systems

Author Keywords
Muscle activation, MMG, vibration, Wearable sensing

INTRODUCTION
Optimal human movement is an important goal for coaches, trainers, therapists and athletes in most sports. This movement is enabled by skeletal muscles which generate the necessary force to aid in locomotion.

To enable favorable skeletal muscle functioning, proper skeletal muscle activation and timing is key. However, injury or poor training habits can lead to sub-optimal timing of muscle activation [20, 34]. Poor timing of activation creates uncoordinated movement strategies which decrease sports performance and increase the risk of injury due to factors such as muscle compensation resulting from muscle imbalance and overuse [13, 19, 29, 34].

Sensing muscle activation in a real world exercise environment is an especially challenging task. This is due to the fact that many exercises and sports involve a high amount body movement due to the high mobility nature of events such as cycling or high impact activities such as jumping. While prior works have explored techniques such as Electromyography (EMG) or Mechanomyography (MMG) [2, 7, 16, 22] in a clinical setting, these approaches are inherently unreliable in high-motion, real-world settings. This is due to motion induced noise (such as impact noise, perspiration, rubbing of sensors and clothing, etc.) common during heavy exercises.

In this paper, we present MyoVibe, our MMG based solution for sensing and predicting individual muscle activation in high motion, high mobility, and high impact movement scenarios. MyoVibe senses and interprets the muscle vibration signal obtained from a wearable sensor network. Based on our modeling of muscle and motion noise, we developed *k-EVA*, a motion artifact mitigation algorithm that alleviates the effect of inertial sensor noise in these high mobility exercises.

In particular, the contributions of our work are threefold:

- We present MyoVibe, a novel vibration-based muscle activation sensing system for use in real world high mobility/ high impact sports and exercise environments.

- We develop a dynamic motion noise mitigation algorithm based on modeling the motion noise characteristics of our vibration signal.

- We design and perform real-world experiments involving exercises with a wide range of muscle activation patterns and motion (such as cycling and jumping, to validate our approach.

To the best of our knowledge, MyoVibe is the first accelerometer-based MMG sensing system that addresses muscle activation sensing in high motion exercises. Our system is able to predict muscle activation with greater than 97% accuracy in static cases and up to 90% accuracy in dynamic exercise environments.

The rest of the paper is organized as follows. Section *System Overview* gives an overview of muscle activation fundamentals and our system. Section *Muscle Activation Detection* describes the details of the MyoVibe system including the *k-EVA* motion artifact reduction method. Section *Experimental Design* presents the experimental setup used to evaluate MyoVibe, including the exercises used, as well as details of our system implementation. Section *Evaluation* presents our results. We discuss related work in Section *Related Work* and finally conclude in Section *Conclusion*.

SYSTEM OVERVIEW
The MyoVibe system infers muscle activation through sensing small muscle vibrations produced when muscles contract.
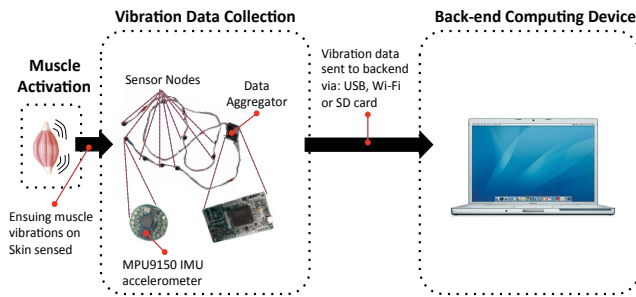
Figure 1. The components involved in the MyoVibe system. The physical system consists of a wearable sensor node network responsible for muscle vibration data collection and a back-end computing device for inferring muscle activation. The sensor node network consists of nodes with mpu9150 accelerometers that sense muscle and a data aggregator.

Through a network of sensor nodes placed on the human body, our system can capture these vibrations. The vibration data are then transmitted to a back-end computing device for processing, where the muscle activation status is inferred from the data. Figure 1 shows an overview of our system. Below, we give a brief introduction of muscle activation theory, the challenges of sensing muscle activation, and the components of the system.

Muscle Activation Background

In this section we provide a brief overview of the physiology of skeletal muscle vibrations that MyoVibe measures.

Skeletal muscles consist of muscle fibers and their associated neurons. The neurons send electric pulses from the brain that cause muscles to contract to enable movement. Prior works using electromyography primarily focuses on measuring these electric signals [2, 16, 22]. However, this approach is more prone to noise because of electrode placement requirements and the lack of direct sensing of body motion. We discuss this related approach in more detail in Section *Related Work*.

During contraction, individual muscle fibers move and rub against each other, creating low amplitude, relatively higher frequency mechanical vibrations [5, 41]. The frequency band in which these vibrations occur is between 5 to 100 Hz, but the exact range varies depending on the particular muscle or type of muscle contraction [3, 4, 7, 41]. This work aims to measure and identify muscle activity directly through these vibrations, or mechamomyography (MMG).

When a skeletal muscle is activated, the signal obtained from that muscle will contain energy in the frequency band at which that muscle vibrates, changing the signal's frequency distribution. By contrast, when muscles are not contracting, the muscle fiber filaments do not rub against each other. Consequently, there are minimal to no ensuing muscle vibrations. It is this change that makes it possible to identify the presence of muscle activation/inactivation.

The Challenge of Sensing Muscle Activation

As described above, an active muscle produces low amplitude high frequency muscle vibrations. This makes measuring muscle activation in a high mobility exercise environment difficult due to the high impact/ high motion noise that activities such as jumping generate. In particular:
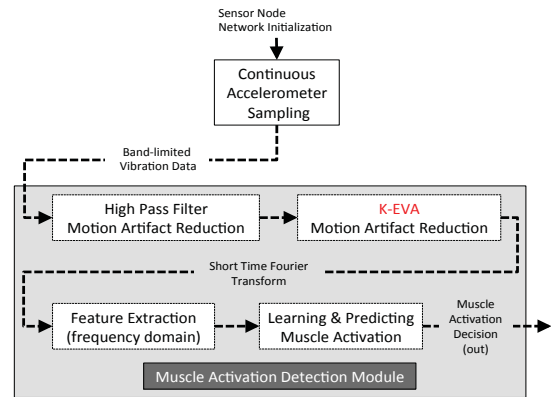

Figure 2. An overview of the flow of information in MyoVibe, our accelerometer-based muscle activation detection system. The system transforms raw band-limited accelerometer data to a muscle activation decision via the muscle activation detection module.

- The sensed signal amplitude that is due to motion is much higher and overwhelms the part that is due to muscle vibrations.

- Non-smooth or impact movements will generate higher frequency components in the sensed signal that overlap with the higher frequency band of the small amplitude muscle vibrations.

As a result, in order to accurately infer muscle activation status, muscle sensing systems need to mitigate this kind of motion noise.

High-pass (HP) filter removes the bulk of the low frequency noise due to body motion [27, 31]. However, the higher frequency components due to the impure nature of body movement that may overlap with the higher frequency muscle vibration signal still remain and pollute the muscle vibration signal. Consequently other techniques are required to limit the higher frequency noise.

In addition to using a HP filter, we developed a novel motion noise mitigation algorithm, *k-EVA*, based on the extreme value analysis (EVA) modeling of vibration data. The *k-EVA* method, is able to reduce such high impact noise and significantly boost muscle activation detection accuracy during high mobility/impact exercises. We describe this motion artifact mitigation technique in detail in Section, *Muscle Activation Detection*.

Vibration Data Collection

MyoVibe relies on a wearable sensor network to collect vibration data and a back-end computing device to process the data. The wearable sensor node network consists of sensor nodes and a data aggregator node. Each sensor node is placed externally on the subjects skin, in the proximity of the muscle to be monitored. Each of the sensor nodes contains a triple axis accelerometer that senses the skeletal muscle vibrations that we described in Section *Muscle Activation Background*.

The sensor nodes are a 2.0 version of the MARS wearable sensor nodes [27]. These sensors have significant reduction in size and weight (36%). This reduction enables the wearable system to be more comfortable and thus, not impede the human subject's motion. In addition, because muscle vibrations produce a force that accelerates the sensor node, a lower
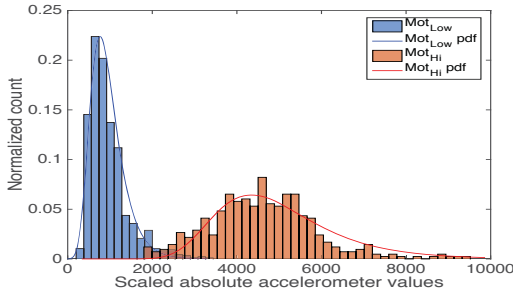
Figure 3. A plot showing the distribution of extreme values in data obtained from activated quadriceps during a low motion isometric leg extension (Mot_{Low} phase) and activated quadriceps during a higher motion squat exercise(Mot_{Hi} phase).The fitted extreme value distributions are shown in blue and red lines respectively.
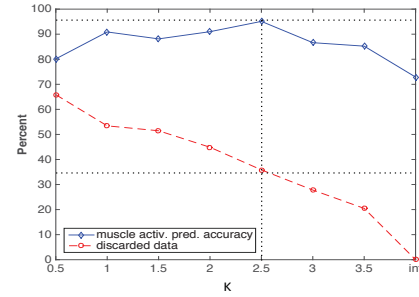

Figure 4. The trade-off between muscle activation prediction accuracy and amount of discarded data when selecting k. The dotted line shows that a value of k≈2.5 provides the highest prediction accuracy (>90%) while discarding about 35% of data.

weight mitigates the distortion of the muscle vibration measured by the sensor node. This makes the system more sensitive to the small muscle vibrations.

Since there are many sensors in close proximity in the sensor node network, the MyoVibe system is connected through a common data bus to a data aggregator node, to minimize interference. The aggregator node coordinates the continuous sampling of the accelerometers in each sensor node. In addition, this node also stores the vibration data locally on an on-board micro-SD, as well as ensures the transmission of vibration data to the backend computing device.

Back-end Computing Device
In order to infer the muscle activation status of a skeletal muscle, MyoVibe relies on a back-end computing device that runs the *Muscle Activation Detection Module*. This module is responsible for converting muscle vibration data into a muscle activation state (inactivated or activated). We further describe this process in Section *Muscle Activation Detection*.

MUSCLE ACTIVATION DETECTION
MyoVibe processes acceleration data and infers muscle activation through the Muscle Activation Detection Module. The processing steps undertaken by this module for such conversion are shown in Figure 2. First, raw band-limited accelerometer data are received and high pass (HP) filtered to reduce noise due to gross motion. Next, the filtered signal undergoes our *k-EVA* motion artifact reduction process. This process identifies and marks high motion noise areas where muscle vibration is likely to be polluted by high motion noise. Next, the muscle activation detection module extracts frequency domain features from the unmarked low motion signals. The features are then used for the initial training of a decision tree model for muscle activation status estimation and prediction.

Motion Artifact Reduction
As mentioned in Section *The Challenge of Sensing Muscle Activation*, the major source of noise in the muscle vibration signal is due to relatively higher amplitude motion noise resulting from both low and high frequency components of body motion. Therefore, by determining the distribution of the high amplitude sensor readings and selectively eliminating them, we can improve the quality of the muscle vibration signal. This is accomplished in our system through both 1) HP filtering and 2) our *k-EVA* Method.

High Pass Filtering: HP filtering is the first step in motion artifact mitigation. This step entails passing all the accelerometer data through a 5Hz HP filter. We use a 5Hz HP filter because applying a cutoff at this point has been shown by previous works to eliminate most of the low frequency noise in accelerometer signal due to gross body motion [7, 31].

***k-EVA* Method:** To mitigate the effect of the relatively higher amplitude and high frequency noise in the sensor data stream, not removed by the HP filter, we developed our *k-EVA* algorithm.

The *k-EVA* algorithm uses extreme value analysis (EVA) to model and separate extreme sensor values (due to motion noise) from lower amplitude muscle vibration sensor values. We use extreme value analysis because body motion will result in higher amplitude "outlier" sensor values than muscle vibrations. By modeling the distribution of the "outliers" and eventually selectively eliminating a majority of these higher/extreme values due to motion noise, MyoVibe can reduce the effect of high motion noise in the accelerometer signal. Specifically, we use the extreme value type I Gumbel distribution to model these values [28]. We used this distribution due to its simplicity and good fit with our data. The parameters of the distribution are obtained using maximum likelihood estimation. Figure 3 shows an example of how actual data fits the distribution.

We model the outlier distribution of muscle vibration during a 20 second low-motion calibration period before each exercises. During this period we collect accelerometer data obtained from a MyoVibe sensor placed on an activated muscle during a low motion (Mot_{Low}) exercise where there is little to no body motion (i.e., isometric exercises). We explain more about these exercises in Section *Experimental Design*.

Once obtained, we divide the data set into successive non-overlapping windows of 500 ms each and record the maximum/extreme values encountered in each window. Using these extreme values, we estimate the scale parameter, σ, of the empirical extreme value distribution underlying the data set. The scale parameter is directly proportional to standard deviation of the distribution. This results in a distribution with a parameter $\sigma_{Mot-Low}$ that describes the extreme values in the low motion phase data. We note here that we did not see a significant change in the EVA distribution when more that 20 seconds worth of calibration data was collected.
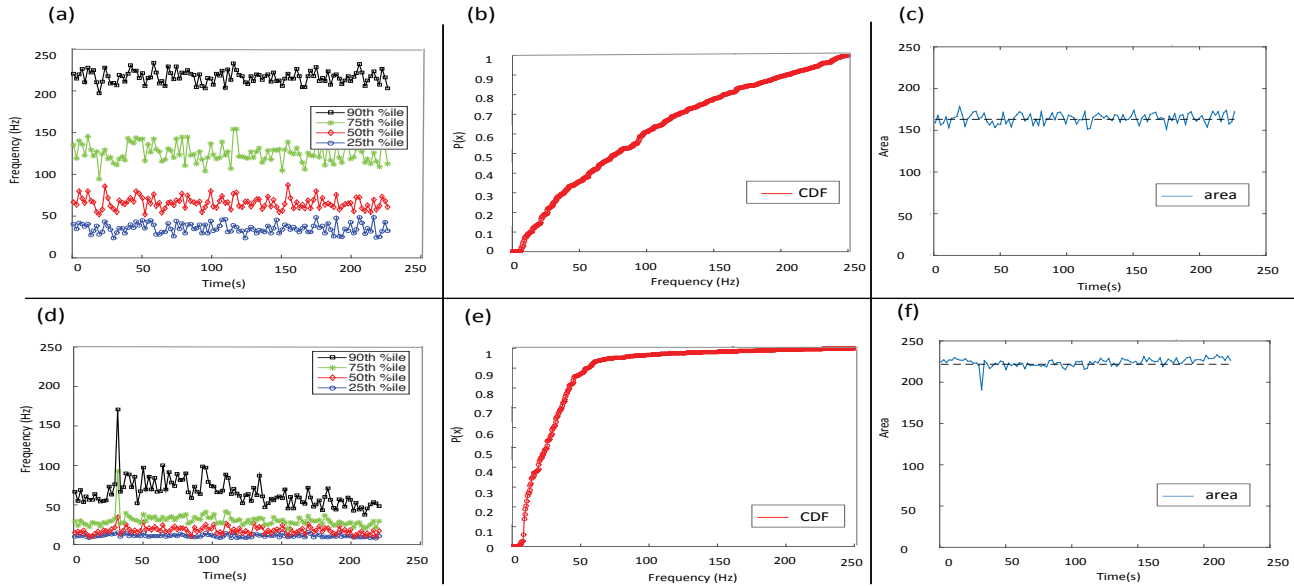
Figure 5. Examples of frequency domain features extracted from the x-axis signal of an accelerometer placed on the quadriceps. Figures (a) and (d) show the percentile frequencies. Figures (b) and (e) show the CDF, and Figures (c) and (f) show the area under the CDF. Figures (a), (b), and (c) show the features for the relaxed case. Figures (d), (e), and (f) show the features for the activated case.

Figure 3 shows a histogram plot of the extreme value distribution obtained from the quadriceps during an isometric leg extension, i.e., the low motion phase, Mot_{Low}. For comparison we also show data collected during a higher motion squat exercise, i.e., a high motion, Mot_{Hi} phase. The figure shows that the extreme values obtained from the Mot_{Low} phase tend to show lower values than those obtained from the Mot_{Hi} phase. Consequently, defining a threshold that separates these two distributions allows our system to identify motion noise from muscle vibration data. This is the threshold that k-EVA determines in the form of a multiplicative constant k multiplied by the $\sigma_{Mot-Low}$ scale parameter.

After the threshold is obtained, the calibration phase is complete. To mitigate motion noise, MyoVibe simply discards any windows of data in the HP filtered data stream that have data points exceeding the k-EVA threshold value.

Caution must be exercised when selecting the value of k to use. k determines the number of 'standard deviations' of the low motion noise EVA distribution to include as muscle activation data. Therefore, if the value of k is too large, more muscle activation data is included, but so is some data from the lower end of the motion noise data. This results in a higher false alarm rate, resulting from muscle activation misclassification errors due motion noise pollution. On the other hand, if the value of k is set too low, whereas the false alarm rate might be low, because the system is too conservative, multiple windows of data and eventually all windows, will be discarded. This trade-off is shown for the squat exercise in Figure 4. In this system, we found k of 2.5 provides a good balance for general motion and the exercises presented in this paper.

We also note here that the k-EVA threshold is determined by the Mot_{Low} phase data. By contrast, any high mobility/high motion exercise will have the higher extreme values, distributed even farther rightward of the Mot_{Low} extreme value

distribution. This means that as long as the k value is set using the above-mentioned guidelines, the type of exercise will not require a change in the threshold value. We show in Section *Evaluation* that using a single well selected k-EVA threshold is effective in removing noise, especially across a variety of high-motion exercises.

Feature Extraction

After motion artifact reduction, the Muscle Activation Detection Module obtains a set of frequency domain features from the accelerometer vibration signal. These features are what our system uses to discern the muscle activation status by quantifying the frequency shifts in the muscle vibration signal, described in the Muscle Activation Background section, that occur when a muscle is activated. We describe these features and the rationale behind them next.

We extract a set of five frequency domain features from each axis of the accelerometer instrumenting every muscle, for a feature vector of dimension 15, $x_i = <x_{i,1}, x_{i,2}, ..., x_{i,15}>$, per accelerometer, placed per muscle. We extract features from each axis so as to capture muscle vibrations regardless of the direction in which they occur. Since the sensor nodes are linked from one node to the other by braided physical wires and woven cloth tape, the axes orientations do not change.

To obtain these frequency domain feature vectors, the muscle activity recognition module calculates a discrete Fourier transform (DFT) of the motion artifact mitigated accelerometer data stream. Next, using a sliding window with a fixed width of 500 ms, our system calculates each respective feature for each accelerometer axis. The result is N observations of the feature vector x_i, where $N = \frac{duration \quad of \quad signal}{window \quad size}$. The features obtained from quadriceps data collected during an isometric (no motion) exercises are shown in Figure 5. The top row Figures 5 (a), (b), and (c) were computed from an in-

active quadriceps muscle. The bottom row Figures 5 (d), (e), and (f) were obtained from an active quadriceps muscle.

The first four features are the $25^{th}, 50^{th}, 75^{th}$ and 90th percentile frequency values. They are shown in Figures 5 (a) and (d) for relaxed and activated cases, respectively. There is a clear downward shift in observed percentile frequencies between the case of relaxed muscle, Figure 5 (a), and activated muscles (during a no motion exercise), Figure 5 (d). We include four percentiles in the feature matrix so as to localize the changes into specific percentile bands. This way, even small local changes in frequency (shifts) are more apparent since they are compared to a local percentile bin as opposed to the entire spectrum.

The fifth feature is the area under the cumulative distribution function (CDF) curve of the frequencies contained in the muscle vibration signal sensed by our accelerometers. The CDF probabilistically defines how all the frequencies contained in the band-limited accelerometer signal are distributed, within a given window. Figures 5 (b) shows the CDF of the frequencies in the signal obtained from inactivated quadriceps muscle. Figure 5 (e) shows the CDF of the frequencies when the quadriceps muscle is activated.

At rest, when the muscle is not actively contracting and/or relaxing, there are minimal to no muscle vibrations sensed by the accelerometer. Consequently, the energy in the accelerometer signal is due to ambient sensor noise and is spread across the entire signal bandwidth, in our case 0-250Hz. As a result, the CDF curve appears closer to the center 1:1 line as in the plot in Figure 5 (b). However, as a muscle becomes activated (no motion exercise case), the sensed signal now contains energy due to muscle vibration and the frequency distribution changes. Since muscle vibrations occur in the 5 to 100Hz frequency range, the signal energy appears to shift to lower frequencies. This means that the CDF curve shifts leftward as shown in Figure 5 (e). This shift also means that the area under the CDF curve increases as shown in Figure 5(f) as compared to the area under the CDF curve when the muscle was relaxed, shown in Figure 5 (c).

These 15 frequency domain feature vectors (5 from each sensing axis) are combined into a single matrix X, shown below of dimension N by M, $M = 15$ on a per muscle basis. This matrix X is the digital representation of the vibration signal that will be used to infer the muscle activation status of an instrumented muscle group.

$$Vibration\ feature \Rightarrow X_{N \times 15} = \begin{pmatrix} x_{1,1} & x_{1,2} & \cdots & x_{1,15} \\ x_{2,1} & x_{2,2} & \cdots & x_{2,15} \\ \vdots & \vdots & \ddots & \vdots \\ x_{N,1} & x_{N,2} & \cdots & x_{N,15} \end{pmatrix}$$

Learning & Predicting Muscle Activation

Once the system has obtained the muscle vibration feature matrix for each of the instrumented muscles, the next step is to build a muscle activation status classifier. The classifier will be trained on labeled vibration feature matrices to provide muscle activation status predictions for future incoming muscle vibration data.

Our system uses supervised machine learning techniques to build the classifier that will infer whether a muscle is activated

or not. In order for the system to match new feature instances to a particular muscle activation status, it must first be trained using a labeled muscle vibration feature matrix, obtained over a specific training period. Therefore, the system requires that each feature instance in the training muscle vibration matrix be labeled as either an inactivated or activated muscle. We accomplish this through an initial training set of exercises in which the ground truth muscle activation status is obtained from a sEMG system.

sEMG is the state-of-the art in muscle activation detection, even though it suffers from motion noise/artifacts from high motion exercises. Therefore, in order to use it, we manually, and with the supervision of a qualified physiotherapist (sEMG expert), process the sEMG data feed to remove these artifacts and get clean ground truth activation data. We describe this process in detail in Section *Obtaining sEMG Ground Truth Labels*.

With this information, the muscle activity recognition module builds a decision tree (DT) classifier which assign labels or muscle identities to new incoming vibration feature data points. We use decision trees because they are sufficient for binary classification, simple and less computationally intensive compered to other more complicated learning algorithms. The DT algorithm learns a hypothesis $h \in H$, (where $H = \{h : h | X \to Y\}$ is the space of all functions that can approximate the target function $f : X \to Y$), to match the muscle vibration feature matrix instances to muscle activation statuses. X in this case is the N by M vibration feature matrix. Y is the vector of muscle activation status, $Y = \{y^{in-activated}, y^{activated}\}$. The function/hypothesis (classifier) h that our system learns will predict a class $y^{in-activated}$ or $y^{activated}$ for a new k^{th} incoming set of feature instances $< x_{k,1}, ...x_{k,M} >$, (M =15), calculated from the accelerometer signal of a muscle of interest. The learned classifier is stored locally on the back-end computing device that hosts the muscle activation detection module in the form of a classifier object.

EXPERIMENTAL DESIGN

In this section, we describe the details of our experiments, including the human subject selection process and the data collection procedures.

Human Subject Selection

In order to test our system, we obtained real world data from six participants who fulfilled the below fitness criteria, three male and three female. The participants were aged between 18 and 45 years of age, exercised regularly, had a maximum blood pressure of 140/80 and a maximum waist size of 100 cm. These criteria were general enough to ensure a wide participant pool but also specific enough to ensure a"fit" testing population, capable of regular physical activity. Participants also had no recent history of lower extremity injuries. This was important for performing lower body exercises. All subject recruitment and participation procedures adhered to and were approved by our institutional review board (IRB).

Sensor Placement

To gather both experimental and ground truth data we used two types of sensors on the participant's legs. The first set were the MyoVibe (accelerometer) sensors, which provided the experimental MMG data. The second set included
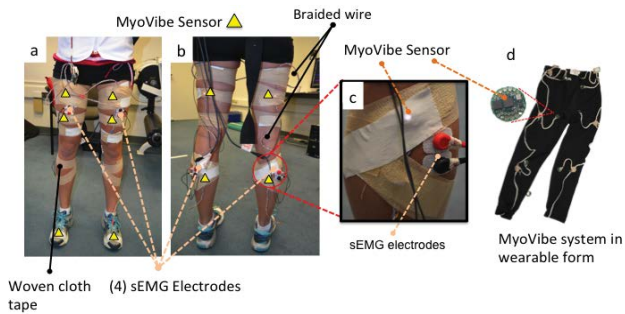
Figure 6. Figures (a) and (b) show the sensor placement for our experiments. Figure (c) shows a close up view of the sensor placement. Figure (d) shows the MyoVibe sensors in wearable form with a close up on the MyoVibe sensor. A total of 10 MyoVibe sensors (yellow triangles) and 4 sEMG sensors were used. Two MyoVibe sensors were placed on each leg's quadriceps. On each foot, and each calf and hamstrings muscle, we placed one MyoVibe sensor. One sEMG electrode was placed on the quadriceps, and calf muscles of each leg. For hygiene reasons, we secured sensors to participants using woven cloth tape instead of using the wearable MyoVibe system.

sEMG sensors, whose data was manually pre-processed by our sEMG expert to produce reliable ground truth muscle activation labels. The sEMG system we used was a 4 channel NeXus-10 Mk I biofeedback system from Mind Media Incorporated [25]. We now describe the sensor setup.

MyoVibe Sensor Setup: We placed a set of five of MyoVibe sensors on the skin, near the center of muscles, on each leg of each participant. As shown in Figure 6, we chose cloth tape to attach MyoVibe sensors to participants rather than use the fitted wearable form shown in Figure 6d, which can also equivalently sense muscle activity [27]. By using cloth tape, we could perform our experiments efficiently and hygienically as the sensors would be easy to remove and clean for use on multiple people. In addition, this way, much like in the fitted clothing case of Figure 6d, neither the sensor orientations nor placement changed during exercise, reducing sensing inconsistencies.

On the quadriceps of each leg we placed two MyoVibe sensors. The hamstrings and calf muscles on each leg, each got one sensor per muscle. We also placed one sensor on each foot of the participant. The foot sensors were used as a reference to automatically detect the active leg during the exercises. This helped to reduce the chances of falsely assigning an 'activated' label to the muscles of an inactive leg and vice-versa.

Each of the MyoVibe sensor nodes contained an Invensense MPU9150 inertial measurement Unit with a triple axis accelerometer, for sensing the muscle vibrations. The accelerometers were sampled at a continuous rate of 500Hz. To band-limit the accelerometer signal, we used the MPU9150's in-built 1st order 98 Hz anti-aliasing low pass filter. MyoVibe sensor nodes are also encased in epoxy, making them sweat and water resistant.

sEMG Sensor Setup: To obtain a ground truth measure of muscle activation, we additionally instrumented each participant's leg muscles with sEMG electrodes. Since we only had a 4 channel sEMG system, we were able to place the electrodes on either the quadriceps or calf of each leg. The sEMG electrodes were placed as close as possible alongside the MyoVibe sensors so as to allow both systems to sense the same
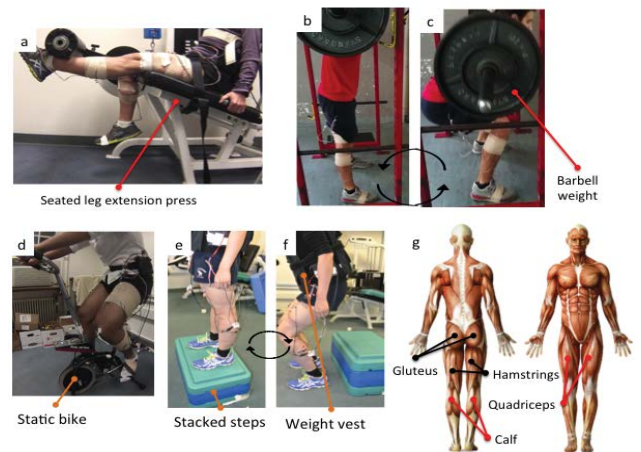

Figure 7. All the exercises investigated in this paper. Figure (a) shows the isometric leg extension. Figures (b) and (c) show the squat. Figure (d) shows the cycling exercise. Figures (e) and (f) show the jumping exercise. Figure (g) shows the muscles worked by these exercises. Table 1 provides more insights and details about these exercises.

muscle. A diagram showing the placement is shown in Figure 6.

To ensure the optimal performance for the sEMG system, our physiotherapist prepared the participants' skin by shaving any hairs and then cleaning the application site with an alcohol prep pad. Once ready, we set the sampling rate of the sEMG machine to the maximum rate of 2048Hz. As a first defense for mitigating noise due to body motion and other sEMG artifacts, all sEMG data was passed through a manufacturer recommended fourth order Butterworth 20Hz - 500Hz bandpass filter. Next we present the exercises which we performed in order to evaluate our system.

Exercise Selection

Since most sport related/exercise muscle injuries occur in lower extremity muscles [9, 11], we centered the evaluation of our system around lower body/leg exercises. Specifically, the exercises that we considered broadly fall into these three categories:

1. Isometric (low motion) exercises

2. Repetitive motion exercises

3. High mobility/high impact exercises

Each exercises was performed for two minutes. We describe each specific exercises in the following sections.

Isometric (low motion) exercise
Isometric exercises are workouts that activate a given muscle in place, consistently for a period of time without resting, and with little to no motion. Thus, they are good muscle isolation exercises. We considered an *isometric leg extension* exercise for this category.

Isometric leg extension: This exercise is shown in Figure 7(a) and works the quadriceps. We selected this exercise so as to test our system in an ideal scenario where the quadriceps muscle activity is isolated from overall body motion.

The exercise involves continuously sustaining a weight with the exercising leg while tensing the quadriceps. So as not to

Figure 7 #	Exercise name	Muscles worked	Details
a	Isometric Leg Extension	Quadriceps	This exercise minimizes motion noise while isolating the quadriceps muscle. Consequently, we could accurately determine MyoVibe's ability to detect muscle activation in the quadriceps.
b,c	Squat	Quadriceps, Hamstrings, Gluteus	The squat allowed us to evaluate our system in a complex, full body free-form exercise that involves slightly more aggressive up and down movement than the isometric exercise.
d	Cycling	Quadriceps, Calf	Cycling provided us with a way to test how well MyoVibe could determine muscle activation in a common, repetitive, yet motion intensive exercise.
e,f	Jumping	Quadriceps	Through this exercise we could test MyoVibe's resilience when used during an ubiquitous exercise that generates an extremely high amount of inertial noise due to intense ground impact.

Table 1. A table containing details about the exercises shown in Figure 7.

over-strain participants but provide adequate resistance, we set the weight to 40% of the maximal voluntary contraction force that the individual could sustain. In order to get sufficient data for analysis, we set the total exercise time to one minute; 30 seconds rest in the beginning, followed by thirty seconds of contraction time.

Repetitive motion exercises
To realistically evaluate our system, we needed to include less ideal and more complex motion exercises than the isometric ones. Consequently, we included repetitive motion exercises such as a *squat* and *cycling* in our evaluation.

Squat: The squat exercise is shown in Figure 7(b,c). The squat works mainly the quadriceps, the gluteus and the hamstrings muscles. We selected the squat because it allowed us to evaluate our system in a complex, full body, free-form exercise that involves more aggressive up and down movement than the isometric exercise. To perform the squat, participants sustained a barbell weight (20% of body mass for men and 12% for women) on their body while repeatedly squatting up and down in a smooth, controlled motion for about two minutes. To ensure consistency among participants, we used an audible metronome set at 30 beats per minute to pace each up/down repetition of the exercise. At rates faster than 30 bpm we found that participants rushed, and broke exercise form. At lower rates, the squat seemed too strenuous for participants, dissuading them from the exercise.

Cycling: The setup for the cycling exercise is shown in Figure 7(d). Cycling works the quadriceps and calf muscles. We selected cycling as a test exercise because we wanted to test how well MyoVibe could determine muscle activation in a common, cyclic and repetitive, yet motion intensive exercise. To perform the exercise, participants got on a stationary bike with adjustable 'exercise resistance'. As the participants began to cycle, we gradually increased the bikes resistance setting (so as to provide adequate exercise intensity), until that participant's pedaling rhythm was stable. This simulated pedaling on a flat road and allowed subjects to pedal with each leg, roughly, every second, ensuring consistency among test participants.

High mobility/impact exercises
To evaluate our system during high mobility/impact exercises, we included a *jumping* exercise. Compared to the repetitive and isometric exercises, jumping has much higher motion noise characteristics due to jump landing impact.

Jumping: The setup of the exercise is shown in Figure 7(f,g). Jumping as an exercise works the quadriceps muscle. We selected this exercise for two main reasons: 1) It generates an extremely high amount of inertial noise from the ground impact of a jump landing. 2) A majority of active sports and exercises involve some form of jumping [14, 30]. Consequently, the ubiquity and robustness of our system depends greatly on the system's ability to detect muscle activation during jumping.

To perform this exercise, participants wore a chest weight vest (to increase resistance and impact noise), got on top of a set of stacked steps (one foot high), and jumped to the ground. To ensure that the quadriceps muscle would be activated, we asked participants to land on the ground in a squatting fashion and hold that position for about one second.

With the selected exercises and muscles worked in mind, we will now evaluate our system's muscle activation detection results during these exercises.

EVALUATION
In this section we present our system evaluation metrics and the results showing the performance of our muscle activation detection system.

A muscle activation result for a participants was determined for each 500 ms window, resulting in roughly 1500 results across all six participants, per exercise. The evaluation metrics we use are precision, recall and accuracy. Precision is the ratio of true positives to that of the sum of true and false positives, or the positive predictive value. Recall is the ratio of true positives to that of the sum of true positives and false negatives or sensitivity. Accuracy is defined as the ratio of the sum of true positives and true negatives to that of the sum of true positives, true negatives, false positives and false negatives. Higher precision, recall and accuracy are better.

In order to calculate these metrics, the muscle activation prediction (activated or not activated) provided by our system needs to be compared to a trusted ground truth label. We use data from a state of the art sEMG machine, as well as involve a trained physiotherapist (sEMG expert), so as to provide accurate ground truth muscle activation labels for a given muscle. We show why a sEMG expert is necessary in the *Jumping exercise results*, subsection. We now briefly describe the method used to obtain the muscle activation labels next.

Obtaining sEMG Ground Truth Labels
The muscle activation ground truth is obtained from the sEMG sensors that instrumented the muscle groups we studied. To get accurate ground truth, we ensured that the sEMG and MyoVibe MMG systems were time synchronised. This
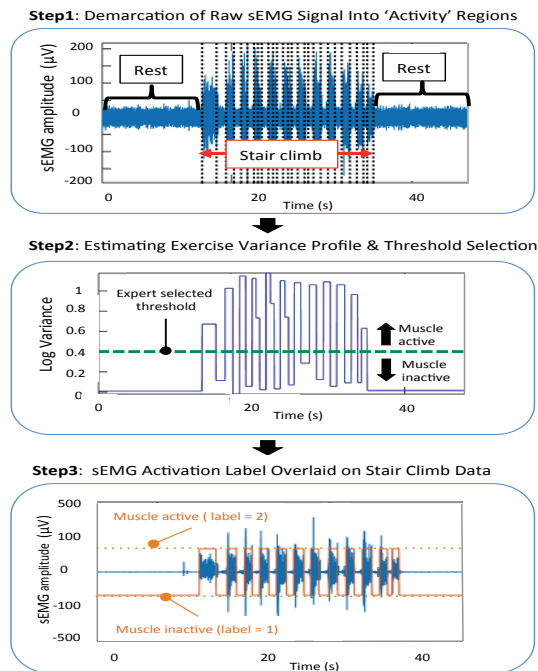
Step1: Demarcation of Raw sEMG Signal Into 'Activity' Regions

Step2: Estimating Exercise Variance Profile & Threshold Selection

Step3: sEMG Activation Label Overlaid on Stair Climb Data

Figure 8. The process of obtaining ground truth labels for calf activation from sEMG data obtained during a stair climb. *Step 1* shows the segmentation of raw sEMG signal into variance based 'muscle activity regions'. *Step 2* shows the variance profile estimated from these regions. Using this variance profile, an expert selects a muscle activation threshold (green dotted line). Finally in *Step3* the threshold is used to assign labels to sEMG data as active(2) or inactive(1).

way, both sensing systems captured the activation state of a muscle at the same point in time.

To obtain muscle activation, we manually processed the sEMG data since sEMG is heavily affected by motion artifacts in high mobility exercises. This meant going through the sEMG data, with the help of a physiotherapist (sEMG expert), and the knowledge of the exercises in question, manually removing areas affected by motion artifact. Once we obtained the processed sEMG data, the next step was to determine whether a muscle is activated or not. For this, we required a muscle activation event detector algorithm to be applied to the expert approved sEMG data.

A common muscle activation event detector algorithm that is in use today and which we apply to our sEMG data, is the *'Moving Average Whitening Filter with Approximate Generalized Likelihood Ratio test decision rule'* (AGLR) algorithm by Staude *et al.* [37, 38, 39]. It determines muscle activation by modeling the digitized sEMG signal as white Gaussian noise with dynamic variance. The sEMG labeling process is shown in Figure 8.

As the muscle moves from an inactive to an active state, the variance in the sEMG signal changes. By windowing the sEMG data and selectively grouping similar variance sEMG windows, we obtain 'muscle activity regions' that demarcate the sEMG data into regions of varying muscle activity. Regions with higher variance, reflect areas of high muscle activity. Low variances mean that little to no activity was detected by the sEMG signal. By extracting a representative measure of the signal variance in each region, a variance profile of the sEMG signal can be obtained.
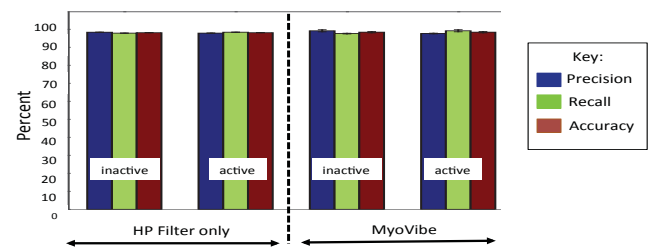

Figure 9. The precision, recall, and accuracy of predicting the activation status (inactive vs. active) of the quadriceps muscle during the no motion isometric leg extension exercise. The results using a high pass (HP) filter only are shown to the left. MyoVibe results are on the right.

Once the variance profile has been obtained, the sEMG expert then manually selects a threshold value based on the exercise. Data points above the threshold are assigned as active (2), while those that are equal to or below the threshold are assigned as inactive (1). This threshold value is based on the sEMG expert's knowledge of the exercise performed and the phase of the exercise during which a muscle of interest was likely activated.

We stress that using a sEMG expert here is paramount. This is so as to have an expert watch out for motion artifacts due to exercise motion, that might result in a high variance signal even when the selected muscle is not activated [32, 33, 43]. Without the human expert intervention, blindly selecting a threshold may lead to mis-labelled data causing erroneous ground truth and system evaluation. We will show results supporting this observation in the high mobility/impact exercise results section.

After the sEMG data has been labeled, denoting whether the muscle was inactive(1) or active(2), the accelerometer sensor data ground truth labels are obtained. Since the sEMG and MyoVibe data were time synchronized, the muscle activity labels transfer directly in time to the accelerometer sensor data. With the ground truth labels now available, we can use our system to infer muscle activation status and determine the accuracy, precision and recall of our entire MyoVibe muscle activation system.

We will now present the muscle activation results obtained using MyoVibe, beginning with the isometric leg extension exercise.

Isometric Leg Extension Evaluation
The muscle activation status prediction results for the isometric leg extension exercise are shown in Figure 9. The results using a high pass (HP) filter only for motion artifact reduction are shown to the left. The results obtained by MyoVibe, when we augment the HP filter with our *k-EVA* motion artifact mitigation method are shown to the right.

The results show that the muscle activation status prediction results using only the standard HP filter approach, show high precision, recall and accuracy $>97\%$. This result does not change when our MyoVibe system *k-EVA* motion artifact mitigation is introduced.

This result is expected as isometric exercises involve very little motion. Therefore a HP filter for reducing signal noise is sufficient to enable accurate muscle activation detection using inertial MMG. Consequently, we can conclude that when there is minimal motion associated with muscle activation,
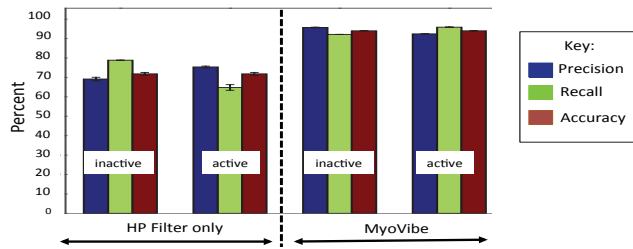
Figure 10. The precision, recall, and accuracy of predicting the activation status (inactive vs. active) of the quadriceps muscle during the squat. High pass (HP) filter only results are on the left. MyoVibe results are on the right. MyoVibe, shows a >20% increase in precision, recall & accuracy. Muscle activation detection error also decreases by 50%.
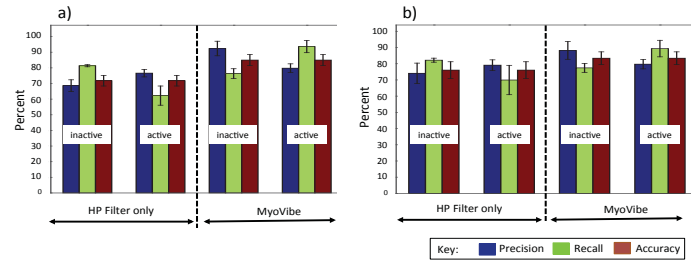

Figure 11. The precision, recall and accuracy of predicting the muscle activation status of the calf (a) and quadriceps muscle (b) during cycling. The (HP) filter only results are shown to the left of either (a) or (b). The MyoVibe *k-EVA* results are shown to the right of (a) and (b). *k-EVA* increases precision by up to 20% and overall accuracy by >10%.

using a HP filter is sufficient for motion noise mitigation. We can also surmise that for the restricted motion exercises, MyoVibe can rival the state-of-the-art sEMG muscle activation system.

Repetitive Motion Exercise Evaluation

In this section we present muscle activation detection prediction results for our MyoVibe system when it is used in the repetitive motion exercises.

Squat Results: The muscle activation determination results for the squat exercise are shown in Figure 10. The results using a standard HP filter are shown to the left. The results obtained using MyoVibe's *k-EVA* are shown to the right. The results differ greatly depending on the motion artifact mitigation method used to process the muscle vibration signal. When using only a HP filter, the precision, recall and accuracy of predicting the inactive/ active state of the muscle lie in the 65-78% range. However, with *k-EVA*, the accuracy of muscle activation detection rises to 93%. This signifies a >20% increase in accuracy and > **50% decrease** in muscle activation detection error.

The squat exercise, involves motion inherent to the exercise itself as well as due to swaying of the barbell or shaking as participants steady themselves during the exercise. This kind of movement is neither regular nor smooth, and results in both low and higher frequency components in the accelerometer signal. Consequently a HP filter alone is an insufficient motion mitigation method. MyoVibe's *k-EVA* method however, significantly improve muscle activation detection. The result is a >50% reduction in prediction accuracy error.

Consequently, we might conclude that during dynamic exercise muscle activation, high pass filtering the accelerometer signal alone is insufficient. By augmenting the HP filter with our *k-EVA* motion artifact reduction algorithm, the accuracy of an inertial muscle activation detection system can be significantly improved.

Cycling Results: The results for predicting the activation status of the muscles used when cycling are shown in Figure 11. Cycling is a high intensity high body motion exercise that we selected to test the ability of MyoVibe to detect muscle activation in simultaneously activated muscle groups, namely the quadriceps and the calf.

Figure 11 shows that for both the calf and quadriceps, the precision and overall accuracy of determining muscle activation status improves by as much as 20% when *k-EVA* is used, as compared to using only the standard HP filter.

Cycling is a noisy exercise in terms of inertial sensor noise because it entails a great deal of motion. Most of this motion is regular, repetitive and cyclical and may be mitigated by a HP-type filter [7]. However, the dynamic nature of cycling introduces other inertial noise due to rubbing of skin or clothing during cycling. This kind of noise may contain broad spectrum high frequency components, not sufficiently eliminated by using a high pass filter. However by using MyoVibe's motion artifact mitigation method, we are able to boost the precision of our system by 10-20% to reach **80-90%**.

High Mobility/Impact Motion Exercise Evaluation

In this section we present the results of our system's prediction of the muscle activation status during exercises that involved a high amount of impact noise and movement related experiment noise.

Jumping Exercise Results: The results for predicting the activation status of the muscles (quadriceps) used during the high mobility jumping exercise are shown in Figure 12. We included this exercise to test MyoVibe's ability to function in a high impact/high mobility noise environment.

The leftmost graph in Figure 12, shows the results obtained using sEMG data in which motion artifacts were not removed by a sEMG expert, compared to the ground truth sEMG data that has been manually pre-screened by the expert. The precision of determining if the quadriceps are in-activated is high but the the recall and overall accuracy are low. The precision for the active case is also low but the recall for this case high. The overall accuracy in both active and inactive cases is low (<65%). Note that this result is actually worse than what is observed when accelerometer based MMG data is processed using only a HP filter (middle graph) and using MyoVibe's (rightmost graph) motion artifact reduction algorithm.

These results arise from the presence of the motion artifact due to the motion noise associated with the initial phase of a jump landing contact, before the quadriceps are activated to stabilize the subject. This initial impact generates high sEMG amplitudes, simulating the result that would be expected if the quadriceps actually activated. Therefore, the threshold selected using the *AGLR* algorithm is misleadingly high, causing the state of the muscle to be erroneously assigned as activated when it actually isn't activated, leading to the lower accuracy.

The middle and rightmost graphs in Figure 12, show the results from the HP and MyoVibe systems respectively. As the
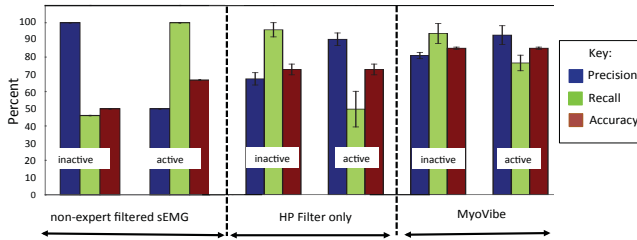
Figure 12. The muscle activation precision, recall and accuracy of the quadriceps muscle during the jumping exercise. The results obtained when using sEMG whose muscle activation thresholds have NOT been pre-screened by a sEMG expert ar shown to the right. The (HP) filter only results are shown in the middle. Finally, the *k-EVA* results are shown to the right. The degradation in unprocessed sEMG due to motion artifact heavily affects muscle activation prediction (<65%) overall accuracy. With *k-EVA*, all the metrics show at least 15% improvement.

results show, when only the HP filter is used, the precision, recall and accuracy of predicting whether the quadriceps are inactive are in the 47% to 82% range. The recall for the active class is especially low at 48%. However, employing the *k-EVA* motion artifact mitigation technique to supplement the HP filter, the precision, recall and accuracy of muscle status prediction are all much higher, ranging from 75% to 88%. This signifies a greater than **50% reduction** in error. This result is especially promising for MyoVibe, given the amount of impact noise that goes along with the jumping exercise and which MyoVibe was able to mitigate to yield the forementioned results.

Having presented our results, we will now discuss related work in the field of muscle activity sensing and muscle activation detection.

RELATED WORK

Whereas MyoVibe is designed for sensing muscle activation in high mobility scenarios, there have been a number of approaches including vision and model based approaches that have been explored [35, 36, 40]. Most model based approaches estimate activity based on motion alone, and thus are not accurate or suitable for fine-grained measurement of muscle activation. Vision based approaches require line of sight to the muscle and are difficult for modern sports where participants are clothed.

For muscle activation sensing, the state-of-the-art is electromyography (EMG) [12, 24]. EMG involves using needle electrodes (fine-wire, EMG) or surface electrodes (surface electromyography or sEMG) to record muscle action potentials. Fine-wire EMG requires a needle to be placed in the muscle being measured. This approach, while accurate, is too invasive for use in an athletic environment. In addition, this method suffers greatly from signal degradation due to motion artifacts when used in a physically active scenario [5, 41].

sEMG is more commonly used since it is less intrusive. We used an expert-aided, sEMG-based ground-truth for our evaluations. However, in general sEMG systems have some limitations. First, electrode placement needs to be precise and largely movement free [10, 15, 17]. In addition, sweat accumulation underneath sEMG electrodes compromises electrode adherence to the skin as well as signal fidelity [2, 16, 22]. Finally, pure sEMG methods cannot directly estimate body motion to combat motion artifact pollution of sEMG

data. These limitations eventually complicate the use of sEMG in high mobility sports.

Currently, there are commercial sEMG systems such as Athos Gear in development for use in exercise environments [1]. In general, the published Athos videos focus on its use in smooth motion squats only, which has well defined motion. In contrast MyoVibe can be utilized in a cases without the assumption of motion. We however, acknowledge that with such advancements in sEMG, both sEMG and MMG systems could possibly supplement each other in a hybrid system and achieve better muscle activity sensing performance.

Aside from EMG, there has also been work that utilizes wearable inertial sensors to measure body motion [6, 26, 42] as well as determine sensor location based on vibration sensing [27]. These works utilize similar sensors used in our system and are complimentary to this work. Recently, some works, including MMG based techniques, have shifted attention to detecting muscle activation in isometric/ (limited to no motion) situations [7, 18, 21, 23]. Unlike EMG approaches, these have the benefit of simplified placement. However, these works still restrict muscle measurements to only static exercise environments on single muscles, since it is easier to sense and infer muscle activation when the signal pollution is low.

Shinohara et al., provided convincing evidence that MMG could be used to monitor quadriceps muscle activation in dynamic exercises with smooth motion such as during cycle ergometry [8]. However, this work involved detecting muscle activation only when maximal contractions (maximum exertion) were involved. This may not always be the case in real-word exercises. In addition, this work does not investigate dynamic high impact events such as jumping. In contrast, the muscle activation results obtained by our system were achieved during sub-maximal muscle contractions, as might be the case during a regular exercise. We also investigate high impact exercises such as jumping that potentially have more signal noise.

CONCLUSION

In this paper we introduced MyoVibe, a system for detecting muscle activation in skeletal muscles during exercises. MyoVibe is a novel inertial mechanomyography-based system that consists of multiple vibration sensors and that utilizes algorithms that account for varying levels of mobility and body motion induced noise. Previous works investigating this subject have focused mainly on single muscle isometric (little to no motion) exercises with little to no signal pollution due to body motion noise.

To the best of our knowledge, our system is the first to addresses the challenges of high mobility exercises and a method that can be implemented across multiple muscles. Specifically, MyoVibe features a *k-EVA* motion artifact reduction technique in addition to HP filtering. This allows our inertial muscle activation detection system to reach the accuracies of more than 98% when detecting isometric low motion exercise muscle activation and >80% when detecting muscle activation in high mobility/noisy environments.

REFERENCES

1. Athos gear and athos core technology. `http://www.liveathos.com/apparel/technology`, 2014. [Online; accessed 27-Feb-2015].

2. Abdoli-Eramaki, M., Damecour, C., Christenson, J., and Stevenson, J. The effect of perspiration on the semg amplitude and power spectrum. *Journal of Electromyography and Kinesiology 22*, 6 (2012), 908–913.

3. Allen, D. G., Lamb, G., and Westerblad, H. Skeletal muscle fatigue: cellular mechanisms. *Physiological reviews 88*, 1 (2008), 287–332.

4. Alves, N., Sejdić, E., Sahota, B., and Chau, T. The effect of accelerometer location on the classification of single-site forearm mechanomyograms. *Biomedical engineering online 9*, 1 (2010), 23.

5. Amft, O., Junker, H., and Lukowicz, P. Sensing muscle activities with body-worn sensors. *Body Sensor* (2006), 6–9.

6. Bao, L., and Intille, S. Activity recognition from user-annotated acceleration data. *Pervasive Computing* (2004), 1–17.

7. Beck, T. W., Housh, T. J., Cramer, J. T., Weir, J. P., Johnson, G. O., Coburn, J. W., Malek, M. H., and Mielke, M. Mechanomyographic amplitude and frequency responses during dynamic muscle actions: a comprehensive review. *Biomed Eng Online 4*, 1 (2005), 67.

8. Bergstrom, H. C., Housh, T. J., Zuniga, J. M., Traylor, D. A., Lewis, R. W., Camic, C. L., Schmidt, R. J., and Johnson, G. O. Mechanomyographic and metabolic responses during continuous cycle ergometry at critical power from the 3-min all-out test. *Journal of Electromyography and Kinesiology 23*, 2 (2013), 349–355.

9. Davies, H., Tietjens, B., Van Sterkenburg, M., and Mehgan, A. Anterior cruciate ligament injuries in snowboarders: a quadriceps-induced injury. *Knee Surgery, Sports Traumatology, Arthroscopy 17*, 9 (2009), 1048–1051.

10. Day, S. Important factors in surface emg measurement. *Calgary: Bortech Biomedical Ltd* (2002).

11. Dixon, J. B. Gastrocnemius vs. soleus strain: how to differentiate and deal with calf muscle injuries. *Current reviews in musculoskeletal medicine 2*, 2 (2009), 74–77.

12. Drost, G., Stegeman, D. F., van Engelen, B. G. M., and Zwarts, M. J. Clinical applications of high-density surface EMG: a systematic review. *Journal of electromyography and kinesiology : official journal of the International Society of Electrophysiological Kinesiology 16*, 6 (Dec. 2006), 586–602.

13. Enoka, R. M., and Duchateau, J. Muscle fatigue: what, why and how it influences muscle function. *The Journal of physiology 586*, 1 (Jan. 2008), 11–23.

14. Fagenbaum, R., and Darling, W. G. Jump landing strategies in male and female college athletes and the implications of such strategies for anterior cruciate ligament injury. *The American Journal of Sports Medicine 31*, 2 (2003), 233–240.

15. Hermens, H. J., Freriks, B., Disselhorst-Klug, C., and Rau, G. Development of recommendations for semg sensors and sensor placement procedures. *Journal of electromyography and Kinesiology 10*, 5 (2000), 361–374.

16. Hunter, A. M., Gibson, A. S. C., Lambert, M. I., Nobbs, L., and Noakes, T. D. Effects of supramaximal exercise on the electromyographic signal. *British journal of sports medicine 37*, 4 (2003), 296–299.

17. Konrad, P. The abc of emg. *A practical introduction to kinesiological electromyography 1* (2005).

18. Kouzaki, M., Shinohara, M., and Fukunaga, T. Non-uniform mechanical activity of quadriceps muscle during fatigue by repeated maximal voluntary contraction in humans. *European journal of applied physiology and occupational physiology 80*, 1 (1999), 9–15.

19. Kumar, S. Theories of musculoskeletal injury causation. *Ergonomics 44* (2001), 17–47.

20. Lucas, K. R., Rich, P. A., and Polus, B. I. Muscle activation patterns in the scapular positioning muscles during loaded scapular plane elevation: the effects of latent myofascial trigger points. *Clinical Biomechanics 25*, 8 (2010), 765–770.

21. Madeleine, P., Jørgensen, L., Søgaard, K., Arendt-Nielsen, L., and Sjøgaard, G. Development of muscle fatigue as assessed by electromyography and mechanomyography during continuous and intermittent low-force contractions: effects of the feedback mode. *European journal of applied physiology 87*, 1 (2002), 28–37.

22. Madler, C., Keller, I., Schwender, D., and Pöppel, E. Sensory information processing during general anaesthesia: effect of isoflurane on auditory evoked neuronal oscillations. *British journal of anaesthesia 66*, 1 (1991), 81–87.

23. Matheson, G., Maffey-Ward, L., Mooney, M., Ladly, K., Fung, T., and Zhang, Y. Vibromyography as a quantitative measure of muscle force production. *Scandinavian journal of rehabilitation medicine 29*, 1 (1997), 29–35.

24. Merletti, R., Botter, A., Troiano, A., Merlo, E., and Minetto, M. A. Technology and instrumentation for detection and conditioning of the surface electromyographic signal: state of the art. *Clinical biomechanics (Bristol, Avon) 24*, 2 (Feb. 2009), 122–34.

25. Mind Media Neuro And Feedback Solutions. *NeXus-10 MK II Biofeedback System*, 10 2014. http://stens-biofeedback.com/products/nexus-10-mark-ii-priced-without-sensors.

26. Moeslund, T. B., Hilton, A., and Krüger, V. A survey of advances in vision-based human motion capture and analysis. *Comput. Vis. Image Underst. 104*, 2 (Nov. 2006), 90–126.

27. Mokaya, F. O., Nguyen, B., Kuo, C., Jacobson, Q., Rowe, A., and Zhang, P. Mars: a muscle activity recognition system enabling self-configuring musculoskeletal sensor networks. In *Proceedings of the 12th international conference on Information processing in sensor networks*, ACM (2013), 191–202.

28. Nadarajah, S., and Kotz, S. The beta gumbel distribution. *Mathematical Problems in Engineering 2004*, 4 (2004), 323–332.

29. Niemeyer, L. O., Aronow, H. U., and Kasman, G. S. A Pilot Study To Investigate Shoulder Muscle Fatigue During a Sustained Isometric Wheelchair-Propulsion Effort Using Surface EMG. *The American journal of Occupational Therapy 58* (2004), 587–593.

30. Olsen, O.-E., Myklebust, G., Engebretsen, L., Holme, I., and Bahr, R. Exercises to prevent lower limb injuries in youth sports: cluster randomised controlled trial. *Bmj 330*, 7489 (2005), 449.

31. Qi, L., Wakeling, J. M., and Ferguson-Pell, M. Spectral properties of electromyographic and mechanomyographic signals during dynamic concentric and eccentric contractions of the human¡ i¿ biceps brachii¡/i¿ muscle. *Journal of Electromyography and Kinesiology 21*, 6 (2011), 1056–1063.

32. Reiss, A., Cheng, J., and Amft, O. Hierarchical motion artefact compensation in smart garments. In *Proceedings of the 2014 ACM International Symposium on Wearable Computers: Adjunct Program*, ACM (2014), 243–248.

33. Ritzmann, R., Kramer, A., Gruber, M., Gollhofer, A., and Taube, W. Emg activity during whole body vibration: motion artifacts or stretch reflexes? *European journal of applied physiology 110*, 1 (2010), 143–151.

34. Shield, A., and Zhou, S. Assessing voluntary muscle activation with the twitch interpolation technique. *Sports Medicine 34*, 4 (2004), 253–267.

35. Sifakis, E., Neverov, I., and Fedkiw, R. Automatic determination of facial muscle activations from sparse motion capture marker data. In *ACM Transactions on Graphics (TOG)*, vol. 24, ACM (2005), 417–425.

36. Sifakis, E., Selle, A., Robinson-Mosher, A., and Fedkiw, R. Simulating speech with a physics-based facial muscle model. In *Proceedings of the 2006 ACM SIGGRAPH/Eurographics symposium on Computer animation*, Eurographics Association (2006), 261–270.

37. Staude, G., and EKG, E. Determination of premotor silent periods from surface myoelectric signals. *Biomed. Tech 45*, 2 (2000), 228–232.

38. Staude, G., Flachenecker, C., Daumer, M., and Wolf, W. Onset detection in surface electromyographic signals: a systematic comparison of methods. *EURASIP Journal on Applied Signal Processing 2001*, 1 (2001), 67–81.

39. Staude, G., and Wolf, W. Objective motor response onset detection in surface myoelectric signals. *Medical engineering & physics 21*, 6 (1999), 449–467.

40. Sueda, S., Kaufman, A., and Pai, D. K. Musculotendon simulation for hand animation. In *ACM Transactions on Graphics (TOG)*, vol. 27, ACM (2008), 83.

41. Tarata, M. T. Mechanomyography versus electromyography, in monitoring the muscular fatigue. *BioMedical Engineering Online 10* (2003), 1–10.

42. Welch, G., and Foxlin, E. Motion tracking: No silver bullet, but a respectable arsenal. *Computer Graphics and Applications, IEEE 22*, 6 (2002), 24–38.

43. Yang, V. X., Gordon, M., Tang, S.-j., Marcon, N., Gardiner, G., Qi, B., Bisland, S., Seng-Yue, E., Lo, S., Pekar, J., et al. High speed, wide velocity dynamic range doppler optical coherence tomography (part iii): in vivo endoscopic imaging of blood flow in the rat and human gastrointestinal tracts. *Optics Express 11*, 19 (2003), 2416–2424.